

# **Finding the arbitrary parameter $L$ in Renormalization Group Theory**

VIA fitting Monte Carlo simulations to Statistical  
Associating Fluid Theory

**Billy Edward Geerhart III**

A project presented for the degree of  
Masters of Science



Department of Physics  
Oregon State University  
August 23, 2016

# **Finding the arbitrary parameter $L$ in Renormalization Group Theory**

VIA fitting Monte Carlo simulations to SAFT

**Billy Edward Geerhart III**

## **Abstract**

I did as I was told.

Things happened as expected

Accept the flat landers universe.

# Contents

<b>1</b>	<b>Introduction</b>	<b>5</b>
<b>2</b>	<b>Methods</b>	<b>7</b>
2.1	Equation Summary . . . . .	7
2.1.1	SAFT-VR EOS with square-well fluids . . . . .	7
2.1.2	Monte Carlo Simulations . . . . .	7
2.2	Partition Function Seperation . . . . .	8
2.2.1	Free Energy via Monte Carlo Simulations . . . . .	8
2.2.2	ideal gas free energy . . . . .	9
2.2.3	hard sphere free energy . . . . .	10
2.2.4	dispersive free energy . . . . .	12
2.3	Computation . . . . .	13
<b>3</b>	<b>Results</b>	<b>16</b>
3.1	Trends in $U, F$ . . . . .	16
3.2	Trends in $S, C_v$ . . . . .	17
3.3	Using Cost to Estimate Best Box Size . . . . .	18
3.4	Coexistence: $T$ vs Density . . . . .	18
<b>4</b>	<b>Conclusion</b>	<b>19</b>
4.1	Conclusion . . . . .	19

# List of Figures

2.1	Caption for this image. . . . .	13
2.2	Here the common tangent method is demonstrated. The free energy at a particular temperature is plotted as a function of density. The two points highlighted by red and blue X's on the curve share a common tangent; this means both points will have the same pressure and chemical potential. The left and right set of plots shows how the signal to noise ratio changes as the temperature increases. Far from the critical point the signal is relatively strong, while the near the critical point the noise becomes significant. To prevent the loss of the signal, first start at a low temperature where the signal is strong. Then gradually increase the temperature while finding common tangents. As the temperature and noise increases, the previous solutions at a slightly lower temperature can be used as a guess for the new higher temperature. . . . .	15
3.1	These graphs show the Monte Carlo simulation results in terms of dispersive free energy and internal energy relative to SAFT at three different box sizes. Both sets of graphs show that a small box size has a higher energy than SAFT, while a larger box will have a lower energy than SAFT. This makes sense because as the box size increases longer wavelength fluctuations are allowed, and these longer wavelengths actually lower the allowed energy as the increase in energy due to the low density regions are more than compensated by the decrease in energy due to the high density regions. Given a constant box size, the high filling fraction simulations cannot fluctuate as much as the low filling fraction simulations, which explains the bulge in the two lower plots. . . . .	16
3.2	These graphs show the Monte Carlo simulations results in terms of dispersive entropy and heat capacity per particle relative to SAFT at three different box sizes. It is interesting to see the entropy trends are nearly the inverse of the heat capacity trends. Both entropy and heat capacity require a derivative to find, it is just that entropy is the negative derivative of Free energy while heat capacity is the positive derivative of internal energy. Given fig. 3.1 showed the internal energy had the same trend as the free energy, it isn't surprising entropy and heat capacity have inverse trends. Regarding the trend itself, the graphs suggest entropy of a small box will have more entropy than SAFT, while a large box will have a lower entropy than SAFT. This trend can be explained by the particles binding together in ways that SAFT could not take into account, and this extra binding will decrease the entropy simply because some states are now favored over other states. . . . .	17
3.3	These graphs show the cost function as a function of the box size for the dispersive free energy, internal energy, entropy, and heat capacity. The cost function is defined as the mean square difference between the Monte Carlo simulations and SAFT evaluated at a filling fraction of [0.15,0.25,0.35,0.45] and evaluated for $0.6 < T < 1.5$ . The dispersive free energy and internal energy show a minimum near $L=7.6$ , while any box size less than $L=8.0$ seems to be just fine for the dispersive entropy and heat capacity. . . . .	18
3.4	Here the gas-liquid coexistence temperature as a function of filling fraction for three different Monte Carlo simulations are compared to SAFT. The box size $L=6.61$ clearly has a higher critical temperature than SAFT, while the box size $L=10.0$ clearly has a lower critical temperature than SAFT. . . . .	18

# Introduction

Outline: Introduction to liquid vapor coexistence Demonstrate the problem Fix the problem what I did

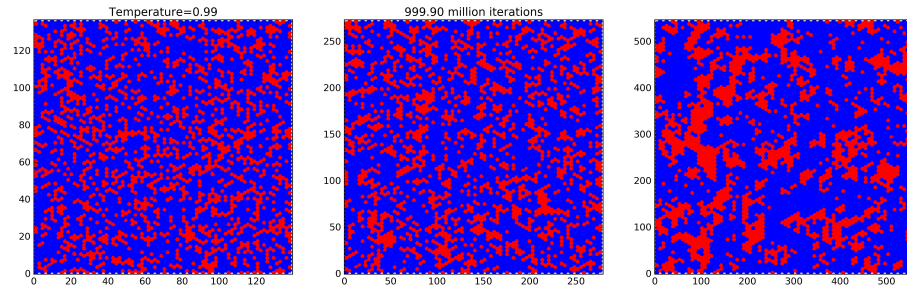
The liquid-vapor phase coexistence can be found by just placing some liquid into a sealed container. Some of the liquid will evaporate into the jar creating a vapor pressure. Provided we placed enough liquid into the jar, the system will now contain both a liquid and a vapor at the same time. By sealing the liquid into a jar, we have forced the pressure of the liquid to be the as the pressure of the gas. By allowing the atoms to swap between the liquid and gas phase, we have also allowed the chemical potential of the liquid to be the same as that of the gas.

Although we can find the phase coexistence by physically sealing a liquid in a jar, an equivalent computational method is to use an empirically determined fluid model which we can use to run simulations that also equalize the pressure and chemical potential. The problem with the computational method is the empirical model requires fitting a few parameters to data, data which probably already includes points on the phase coexistence curve. The main benefit to the computational approach is that once the empirical parameters are found, we can then create the phase coexistence of a mixture of fluids using the previously determined parameters.

One of the difficulties with the computer simulations is computation time. A simulation with a handful of atoms can be finished within 20 minutes, yet a simulation with a 100 atoms can take as long as 4 days. To recreate the phase coexistence graph requires setting the pressure and chemical potential of both phases equal to each other, but this is equivalent to plotting the free energy as a function of density and searching for a common cotangent. For even a simulation that uses a small box, the problem is plotting free energy as a function of density requires many simulations at various densities; some simulations containing only a handful of atoms while other simulations containing as much as a couple hundred atoms. Total computation time for 10 computer cores to create the free energy as a function of density graph can take as long as three weeks.

Naturally there is a tradeoff between a realistic computation time for a project and how realistic the results are going to be. The simulations use periodic boundary conditions which is just the thermodynamic way of saying the boundary should not affect the bulk properties. The key part being whatever is in the simulation is considered the bulk, which is a problem since a small simulation can hardly be considered the bulk. To get around this problem, the simulation size is usually increased until the simulation does represent the bulk.

Normally increasing the simulation size is just fine, but there is a regime where the bulk properties depend on length scales of the order of a millimeter. This regime occurs near the critical point where the liquid density approaches that of the vapor. Normally the liquid and vapor are entirely separated due to the surface tension. However; as the system approaches the critical point, the surface tension approaches zero which means the liquid and vapor will start to mix. Although figure 1 shows an extreme example of a liquid completely mixing with vapor, even under normal circumstances there exist natural fluctuations in the density of either phase. It just so happens that these fluctuations are significant as the density of the liquid approaches the density of the gas at the critical point. Basically the fluctuations within each phase would normally be rather small, but near the critical point the fluctuations are relatively big since the gas and liquid phases are morphing into each other. This is a problem since it requires the simulations to be about the same size as that of the largest fluctuation. For example, a 1mm length box would contain roughly  $10^{19}$  atoms, which would require an unfeasible computation time.



Renormalization group theory(RGT) can be applied to get around this large fluctuation problem. Simply put, RGT is a method in which fine details are omitted from calculations while still maintaining accuracy. This is done by transforming the original partition function into a smaller partition function, but the smaller system is renormalized to the original partition function. [add details...]

In particular, RGT is applied through an interaction wave length. The zeroth order is just the ideal gas term in which all atoms only interact with the walls of the enclosure. The next order is applied via SAFT-VR in which a mean interaction and an approximate wavelength interaction is applied. Longer wavelength interactions can then be applied using RGT via a iterative method that steadily increases the size of the box.

The main problem this project addresses is the transition from SAFT-VR to the application of RGT. Within RGT there is an arbitrary base wavelength  $L$  which is usually fit to the data. However; this arbitrary wavelength shouldn't really be an arbitrary parameter as SAFT-VR already includes interactions at some unknown wavelength. This project attempts to find the base wavelength that SAFT-VR implements, and tests how the results of RGT change when using this base wavelength.

The base wavelength is found by using Monte Carlo Markov Chain (MCMC) simulations at various box sizes. The idea is that a MCMC simulation using a fixed box size of  $L_0$  will incorporate interactions at this box size. The box size is then varied until the results from the MCMC simulations fit the results from SAFT-VR. Once the optimal box size is found, RGT is implemented using this optimal box size and the results are compared to previous results.

# Methods

The methods section is partitioned into theory, which define the equations used, and the actual implementation through computational techniques. The main point of the theory is to estimate the free energy  $F$  from which any of the thermodynamic variables can be found. For example, the entropy, chemical potential, or pressure can be found by the differential  $dF = -S \cdot dT - P \cdot dV + \mu \cdot dN$ . Further, the internal energy can be found by  $U = F + T \cdot S$ . Once the free energy is found, the next goal is to fit the Monte Carlo simulations to SAFT by using a cost function that compares each thermodynamic variable from the Monte Carlo simulations to SAFT. The comparisons are constrained to a temperature range of  $0.45 < T/T_c < 1.13$  where  $T_c$  is the critical point using SAFT; the lower bound is chosen mostly to decrease the computation time of the simulations, while the upper limit is chosen to stay away from the well known hard sphere behavior. To decrease computation times even further, the comparisons are again constrained to filling fractions of  $[0.15, 0.25, 0.35, 0.45]$ . Once the cost can be determined, a 'best' box size is chosen that decreases the overall cost. The final step is to compare this best box size to slightly larger and smaller box sizes by looking at the coexistence densities of the liquid and gas phases.

## Equation Summary

### SAFT-VR EOS with square-well fluids

$$\frac{F}{N \cdot k \cdot T} = a^{HS} + \beta \cdot a_1^{SW} + \beta^2 \cdot a_2^{SW} \quad (2.1) \quad n_{eff} = c_1 \cdot n + c_2 \cdot n^2 + c_3 \cdot n^3 \quad (2.6)$$

$$a^{HS} = -\ln(1 - 4 \cdot n) \quad (2.2)$$

$$a_1^{SW} = a_1^{VDW} \cdot g^{HS}(1; n_{eff}) \quad (2.3) \quad \begin{pmatrix} c_1 \\ c_2 \\ c_3 \end{pmatrix} = \begin{pmatrix} 2.25855 & -1.50349 & 0.249434 \\ -0.669270 & 1.40049 & -0.827739 \\ 10.1576 & -15.0427 & 5.30827 \end{pmatrix} \times \begin{pmatrix} 1 \\ \lambda \\ \lambda^2 \end{pmatrix} \quad (2.7)$$

$$a_1^{VDW} = -4 \cdot n \cdot \epsilon \cdot (\lambda^3 - 1) \quad (2.4) \quad a_2^{SW} = \frac{1}{2} \cdot \epsilon K^{HS} n \cdot \frac{\partial a_1^{SW}}{\partial n} \quad (2.8)$$

$$g^{HS}(1; n_{eff}) = \frac{1 - n_{eff}/2}{(1 - n_{eff})^3} \quad (2.5) \quad K^{HS} = \frac{(1 - n)^4}{1 + 4 \cdot n + 4 \cdot n^4} \quad (2.9)$$

### Monte Carlo Simulations

$$Z = Z_{ideal} \cdot Z_{HS} \cdot Z_{disp}$$

$$Z_{ideal} = V^N \cdot \frac{1}{N!} \int \dots \int e^{-\beta \cdot [P_1^2/2m + P_2^2/2m + \dots]} d\vec{P}_1 \cdot d\vec{P}_2 \dots d\vec{P}_N$$

$$Z_{HS} = e^{-S_{exc.\infty}/k}$$

$$Z_{disp} = \frac{Z_{interaction}}{Z_{HS}} = \frac{\sum_i \alpha \cdot D(E_i) \cdot e^{-\beta \cdot E_i}}{\lim_{T \rightarrow \infty} \sum_i \alpha \cdot D(E_i) \cdot e^{-\beta \cdot E_i}} = \frac{\sum_i D(E_i) \cdot e^{-\beta \cdot E_i}}{\sum_i D(E_i)}$$

where  $S_{exc.\infty} = k \cdot \ln(P_{success})$  and  $P_{success}$  is the probability of a successful attempt to scale an infinite box down to the size of the actual box of the simulation without hard sphere collisions; this shrinking can be done in small steps and the net sum in the change in entropy is then  $S_{exc.\infty}$ .

## Partition Function Seperation

The partition function can be partitioned into high and low temperature regimes. At low temperatures the interactions dominate, while at high temperatures the system acts like a hard sphere system in which the entropy dominates. Both regimes can be partitioned yet again by seperating the kinetic energies into an ideal gas term. In terms of equations, we start with the partition function and seperate the summation into the three partitions:

$$Z = \frac{1}{N!} \sum_i e^{-\beta \cdot E_i} Z = \frac{1}{N!} \int \dots \int e^{-\beta \cdot [\{P_1^2/2m + P_2^2/2m + \dots\} + V(\vec{R}_1, \vec{R}_2, \dots)]} d\vec{P}_1 \cdot d\vec{P}_2 \dots d\vec{P}_N \cdot d\vec{R}_1 \cdot d\vec{R}_2 \dots d\vec{R}_N$$

The momentum integrals are independent of the position integrals, so we seperate the momentum integrals which we then incorporate into an ideal gas term by multiplying by  $V^N/V^N$ .

$$Z = Z_{ideal} \cdot \frac{1}{V^N} \cdot \int \dots \int e^{-\beta \cdot V(\vec{R}_1, \vec{R}_2, \dots)} d\vec{R}_1 \cdot d\vec{R}_2 \dots d\vec{R}_N$$

where

$$Z_{ideal} = V^N \cdot \frac{1}{N!} \int \dots \int e^{-\beta \cdot [P_1^2/2m + P_2^2/2m + \dots]} d\vec{P}_1 \cdot d\vec{P}_2 \dots d\vec{P}_N$$

After taking into account the ideal gas term, the remaining potential energy term is seperated into the low temperature and high temperature regime. At high temperatures, the atom energies are much higher than the potential well; this means the finite potential well can be considered zero. However; even at infinite temperature the atoms are assumed to be a hard sphere. This hard sphere behavior is incorporated into the partition function by multiplying by  $Z_{HS}/Z_{HS}$ .

$$Z = Z_{ideal} \cdot Z_{HS} \cdot \frac{1}{Z_{HS}} \cdot \frac{1}{V^N} \cdot \int \dots \int e^{-\beta \cdot V(\vec{R}_1, \vec{R}_2, \dots)} d\vec{R}_1 \cdot d\vec{R}_2 \dots d\vec{R}_N$$

$$\text{where } Z_{HS} = \frac{1}{V^N} \int \dots \int e^{-\beta \cdot V_{HS}(\vec{R}_1, \vec{R}_2, \dots)} d\vec{R}_1 \cdot d\vec{R}_2 \dots d\vec{R}_N$$

After taking into account the high temperature hard sphere behavior, the last part is just the ratio between the interaction and the hard sphere partition function; we call this the dispersive term.

$$Z = Z_{ideal} \cdot Z_{HS} \cdot \frac{Z_{interaction}}{Z_{HS}} = Z_{ideal} \cdot Z_{HS} \cdot Z_{disp}$$

$$\text{where } Z_{interaction} = \frac{1}{V^N} \cdot \int \dots \int e^{-\beta \cdot V(\vec{R}_1, \vec{R}_2, \dots)} d\vec{R}_1 \cdot d\vec{R}_2 \dots d\vec{R}_N$$

$$\text{and } Z_{disp} = \frac{Z_{interaction}}{Z_{HS}}$$

## Free Energy via Monte Carlo Simulations

[FIX INTRO] Given the separated partition function, the free energies are just the sum of the free energies due to the ideal term, the hard sphere term, and the dispersive term. The ideal term is ignored because it stays the same between theory



and the Monte Carlo simulations. Due to the finite nature of the Monte Carlo simulations, the hard sphere term in the simulations aren't exactly the hard sphere terms in theory. Although we can make some corrections due to the finite nature, ultimately we have to enforce the boundary condition that at high temperature the atoms behave like hard spheres. Given this boundary condition, we are then able to define what the dispersion term should be based on estimation of the density of states.

## ideal gas free energy

To find the ideal gas free energy we can use previous results based on knowing the entropy of the system which we can then use to find  $F_{ideal} = U_{ideal} - T \cdot S_{ideal}$ .

$$U_{ideal} = 3/2 \cdot N \cdot k \cdot T$$

$$S_{ideal*} \approx k \cdot N \left( \ln \left[ \frac{V}{N} \left( \frac{4 \cdot \pi \cdot m}{3 \cdot h^2} \cdot \frac{U}{N} \right)^{3/2} \right] + \frac{5}{2} \right)$$

The Sackur-Tetrode equation with the Stirling approximation actually does not make physical sense as the entropy per particle at constant temperature only depends on density. A simple example can show why this doesn't make sense. Consider two atoms in boxes separated by a partition, and compare the entropy per particle to when the partition in the box has been removed. Once the partition has been removed, the two atoms can explore many more configurations than previously, which means the entropy should have increased once the two atoms were allowed to mix. Unfortunately the Sackur-Tetrode equation with Stirlings approximation would predict the entropy per particle with or without the partition should be the same. This is a bit of a problem since every box in a Monte Carlo simulation will contain exactly N particles, which means the entropy is actually lower than a real ideal gas.

The entropy problem can be fixed by using the Sackur-Tetrode equation without Stirling's approximation. Essentially use a constant density and compare the entropy per particle of a small box to the entropy per particle of a large box. The difference in entropy shows how the ideal gas entropy within a box will deviate from the expected ideal gas entropy.

$$S_{ideal} = k \cdot N \left( \ln \left[ V \cdot N!^{-1/N} \left( \frac{4 \cdot \pi \cdot m}{3 \cdot h^2} \cdot \frac{U}{N} \right)^{3/2} \right] + \frac{3}{2} \right)$$

It would be natural to think we can just incorporate this deviation in entropy for the Monte Carlo simulations, unfortunately the simulations contain an intractable problem involving the periodic nature of the simulations. The atoms in the box are repeated in a periodic way to represent the atoms in the entire fluid, however by forcing a periodic boundary condition the entire state of a fluid is now defined by only the atoms within the small box. It is very unlikely that 100 atoms can fully define a system containing an Advogadro's number of atoms, so the entropy should be much less than a realistic system. Rather than incorporate such a change in entropy, we must instead recognize that bulk properties shouldn't depend on the boundary conditions. By applying periodic boundary conditions we are considering the small box to be the bulk.

Although the small box does not represent the bulk, SAFT also contains the problem of using the small system to represent the bulk. Yet SAFT also enforces the boundary conditions that at high temperatures the fluid should behave like a hard sphere fluid. As such the Monte Carlo simulations are also assumed to behave like a hard sphere fluid at high temperatures, which includes both the ideal term and the hard sphere term.

## hard sphere free energy

The hard sphere partition function can be found by calculating the excess entropy at  $T \rightarrow \infty$ . This can be seen as follows:

$$\begin{aligned}
 Z_{exc} &= Z_{HS} \cdot Z_{disp} \Rightarrow \\
 F_{exc} &= -k \cdot T \cdot \ln(Z_{exc}) = -k \cdot T \cdot \ln(Z_{HS}) - k \cdot T \cdot \ln(Z_{disp}) \Rightarrow \\
 S_{exc.\infty} &= \lim_{T \rightarrow \infty} - \left( \frac{\partial F_{exc}}{\partial T} \right)_{V,N} \quad \text{but} \quad \lim_{T \rightarrow \infty} Z_{exc} = \text{constant} \Rightarrow \\
 S_{exc.\infty} &= -k \cdot \ln(Z_{HS.\infty}) - k \cdot \ln(Z_{disp.\infty}) \\
 \text{but } Z_{HS} &\text{ is constant and } Z_{disp.\infty} = Z_{interaction.\infty}/Z_{HS} = Z_{HS}/Z_{HS} = 1 \Rightarrow \\
 S_{exc.\infty} &= -k \cdot \ln(Z_{HS}) - k \cdot \ln(1) = -k \cdot \ln(Z_{HS}) \Rightarrow \\
 Z_{HS} &= e^{-S_{exc.\infty}/k}
 \end{aligned}$$

To find the hard sphere partition function, we need to find the maximum excess entropy as  $T \rightarrow \infty$ . The method used to find the maximum excess entropy starts by considering N atoms in an extremely large box at a very large temperature. The atoms in the large box should behave like an ideal gas, so the entropy of this large box is a known starting point. Then all atom positions are scaled relative to a corner as the origin. Although each individual atom can now exist within a smaller box, it is not guaranteed an atom will not overlap with another atom after the positions are scaled down.

What we can observe is the probability that a particular scaling fails, and from this probability the change in entropy from the bigger box down to the smaller box can be calculated. The details are as follows:

$$\begin{aligned}
 F &= U - T \cdot S \Rightarrow S = (U - F)/T \approx -F/T = k \cdot \ln(Z) \\
 \text{let } Z_{small} &= \text{partition function of the smaller box} \\
 \text{let } Z_{big} &= \text{partition function of the bigger box} \\
 \Delta S &= S_{small} - S_{big} = k \cdot \ln(Z_{small}) - k \cdot \ln(Z_{big}) = k \cdot \ln(Z_{small}/Z_{big})
 \end{aligned}$$

From here note that although every configuration in the bigger box is not guaranteed to scale down into the smaller box, it is guaranteed that the smaller box can be expanded into the bigger box. This means there is a mapping from the partition function in the smaller box to the bigger box; as such we can break  $Z_{big}$  into valid and invalid configurations where the valid configurations are guaranteed to shrink down into the smaller box and the invalid configurations are not. The  $\Delta S$  can then be simplified by making a connection between  $Z_{small}$  and  $Z_{valid}$ .

$$\text{let } Z_{big} = Z_{valid} + Z_{invalid}$$

but  $Z_{small}$  maps into  $Z_{valid} \Rightarrow Z_{small} = \alpha \cdot z_{valid}$  for some constant  $\alpha$

This constant  $\alpha$  can be found directly by looking at the partition function of both the big and small box. All configurations in the small box can be mapped into the valid regions of the large box which means to find  $\alpha$  all we have to do is rewrite  $Z_{small}$  in terms of  $Z_{big}$ .

$$Z_{small} = \frac{1}{N!} \int \dots \int e^{-\beta \cdot [P_1^2/2m + P_2^2/2m + \dots] + V(\vec{R}_1, \vec{R}_2, \dots)} d\vec{P}_1 \cdot d\vec{P}_2 \dots d\vec{P}_N \cdot d\vec{R}_1 \cdot d\vec{R}_2 \dots d\vec{R}_N$$

The momentum integrals are assumed independent of the spatial integrals, so we can leave them out of the comparison.

$$Z_{small} \propto \frac{1}{N!} \int \dots \int e^{-\beta \cdot [V(\vec{R}_1, \vec{R}_2, \dots)]} d\vec{R}_1 \cdot d\vec{R}_2 \dots d\vec{R}_N$$

From here make the change of variables for each spatial coordinate to remap the integral from the small partition function into the big partition function, and in the process the scaling term  $\alpha$  is found.

$$Z_{small} \propto \frac{1}{N!} \int \dots \int e^{-\beta \cdot [V(\vec{R}_1, \vec{R}_2, \dots)]} d\vec{R}_1 \cdot \left(\frac{L_{big}}{L_{small}}\right)^3 \cdot d\vec{R}_2 \cdot \left(\frac{L_{big}}{L_{small}}\right)^3 \dots d\vec{R}_N \cdot \left(\frac{L_{big}}{L_{small}}\right)^3 \cdot \left(\frac{L_{small}}{L_{big}}\right)^{3N}$$

$$Z_{small} = \left(\frac{L_{small}}{L_{big}}\right)^{3N} \cdot Z_{big} = \left(\frac{V_{small}}{V_{big}}\right)^N \cdot Z_{big} \doteq \alpha \cdot Z_{big} \Rightarrow$$

$$\alpha = (V_{small}/V_{big})^N$$

Now that  $\alpha$  is known, we can get back to finding the entropy.

$$\Delta S = k \cdot \ln(Z_{small}/Z_{big}) = k \cdot \ln(\alpha \cdot Z_{valid}/Z_{big})$$

$$\Delta S = k \cdot \ln\left(\frac{V_{small}^N}{V_{big}^N} \cdot Z_{valid}/Z_{big}\right)$$

but  $Z_{valid}/Z_{big}$  = probability of success when scaling =  $P_{success} \Rightarrow$

$$\Delta S = k \cdot \ln\left(\frac{V_{small}^N}{V_{big}^N} \cdot P_{success}\right)$$

At this point this  $\Delta S$  represents the total change in entropy from squeezing the box. However; only the change in excess free entropy was wanted. To compensate, simply subtract the change in entropy due to the ideal gas using constant temperature and constant number of atoms.

$$\Delta S_{exc.\infty} = \Delta S_{\infty} - \Delta S_{ideal.\infty}$$

$$\text{but } \Delta S_{ideal.\infty} = k \cdot N \cdot \ln(V_{small}/V_{big}) \Rightarrow$$

$$\Delta S_{exc.\infty} = k \cdot \ln\left(\frac{V_{small}^N}{V_{big}^N} \cdot P_{success}\right) - k \cdot N \cdot \ln(V_{small}/V_{big})$$

$$\Delta S_{exc.\infty} = k \cdot \ln(P_{success})$$

## dispersive free energy

The dispersive term is found by estimating the density of states using a \* method. The main problem is the density of states is found by sampling the energy levels, but the relative distribution of energy levels is not unique to a single density of states. In other words, the partition function can be changed by an arbitrary factor without actually changing the total energy. This can be seen as follows:

Suppose

$$Z = \sum_i D(E_i) \cdot e^{-\beta \cdot E_i}$$

then

$$U = \sum_i E_i \cdot D(E_i) \cdot e^{-\beta \cdot E_i} / Z$$

Now suppose we let

$$D_2(E_i) = \alpha \cdot D(E_i)$$

then

$$Z_2 = \sum_i \alpha \cdot D(E_i) \cdot e^{-\beta \cdot E_i} = \alpha \cdot Z \Rightarrow$$

$$U_2 = \sum_i E_i \cdot D_2(E_i) \cdot e^{-\beta \cdot E_i} / Z_2$$

$$U_2 = \sum_i E_i \cdot \alpha \cdot D(E_i) \cdot e^{-\beta \cdot E_i} / (\alpha \cdot Z)$$

$$U_2 = \sum_i E_i \cdot D(E_i) \cdot e^{-\beta \cdot E_i} / Z$$

$$U_2 = U$$

Basically the partition function will define the total energy at all temperatures, but knowing the total energy at all temperatures will not define a unique partition function. Specifically, the partition function up to some arbitrary factor will give the same total energy. This is a bit problematic considering the method to find the density of states makes observations of the total energy to estimate the density of states, which then results in a density of states that is only defined up to some unknown factor.

To get around this problem of an unknown factor in the density of states, note that the dispersive partition function will go towards one as T approaches infinity. This happens because  $Z_{disp}$  is the ratio of the interaction term to the hard sphere term, and the interaction term approaches the hard sphere term as the temperature increases. Essentially we can leave the unknown  $\alpha$  term alone, and it will show up in both the interaction and hard sphere partition function.

That is:

$$Z_{disp} = \frac{Z_{interaction}}{Z_{HS}} = \frac{\sum_i \alpha \cdot D(E_i) \cdot e^{-\beta \cdot E_i}}{\lim_{T \rightarrow \infty} \sum_i \alpha \cdot D(E_i) \cdot e^{-\beta \cdot E_i}} = \frac{\sum_i D(E_i) \cdot e^{-\beta \cdot E_i}}{\sum_i D(E_i)}$$

## Computation

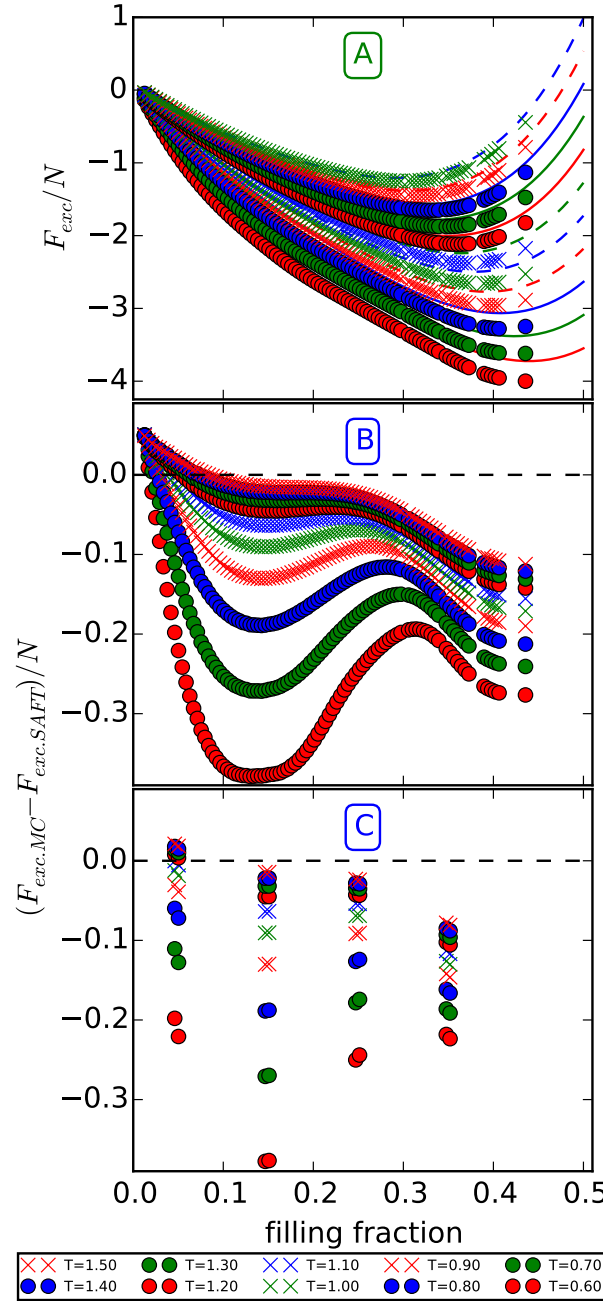


Figure 2.1: Caption for this image.

which At phase coexistence we want  $\mu_{liquid} = \mu_{gas}$  and  $P_{liquid} = P_{gas}$ , so provided we know free energy we can simply find coexistence by setting the following:

$$\mu = \left( \frac{\partial F(T, V1, N)}{\partial N} \right)_{T, V1} \Big|_{N1} = \left( \frac{\partial F(T, V1, N)}{\partial N} \right)_{T, V1} \Big|_{N2} \quad (2.10)$$

$$P = \left( \frac{\partial F(T, V, N1)}{\partial V} \right)_{T, N1} \Big|_{V1} = \left( \frac{\partial F(T, V, N2)}{\partial V} \right)_{T, N2} \Big|_{V2} \quad (2.11)$$

Notice that one set of derivatives are at constant V while the other set of derivatives are at constant N. Luckily this means we can simplify the derivatives by instead

considering the free energy per volume; the reason this helps is both the free energy and volume are extensive quantities, which means the ratio  $F/V$  must be an intensive quantity which further means  $F/V = f$  must only depend on intensive parameters. I.e.  $F(T, N, V)/V = f(T, N/V) = f(T, n)$ . First start simplifying eq. 2.10 by:

$$\mu = \left( \frac{\partial F(T, V, N)}{\partial N} \right)_{T, V} \cdot \frac{V}{V} = \left( \frac{\partial (F(T, V, N)/V)}{\partial (N/V)} \right)_{T, V} = \left( \frac{\partial f(T, n)}{\partial n} \right)_{T, V} \quad (2.12)$$

At this point we know  $\mu_1 = \mu_2$  which combined with eq. 2.12 just indicates that if we plotted the free energy as a function density, then coexistence must occur when the instantaneous slope at one density matches the instantaneous slope at another density. This is useful to know, but it isn't enough to pin down a unique coexistence point. As such we must move on to simplifying eq. 2.11:

$$P = \left( \frac{\partial F(T, V, N) \cdot V/V}{\partial V} \right)_{T, N} = \left( \frac{\partial f(T, n) \cdot V}{\partial V} \right)_{T, N} = f + V \cdot \left( \frac{\partial f(T, n)}{\partial V} \right)_{T, N} \quad (2.13)$$

To simplify the last partial, use the cyclic chain rule by holding T constant throughout the process while considering the set of variables  $(f, N, V)$ . Proceed as follows:

$$\begin{aligned} \left( \frac{\partial X}{\partial Y} \right)_Z \cdot \left( \frac{\partial Y}{\partial Z} \right)_X \cdot \left( \frac{\partial Z}{\partial X} \right)_Y &= -1 \rightarrow \\ \left( \frac{\partial f(T, n)}{\partial V} \right)_{N, T} \cdot \left( \frac{\partial V}{\partial N} \right)_{f(T, n), T} \cdot \left( \frac{\partial N}{\partial f(T, n)} \right)_{V, T} &= -1 \end{aligned} \quad (2.14)$$

But we can simplify the last partial since from eq. 2.12 we already know that  $\left( \frac{\partial N}{\partial f(T, n)} \right)_{V, T} = \frac{V}{\mu}$ . Further, we can simplify the middle partial by noting  $f(T, n) = \text{constant} \Rightarrow f(T, N/V) = \text{constant} \Rightarrow N/V = \text{constant} \Rightarrow \left( \frac{\partial V}{\partial N} \right)_{f(T, n), T} = \frac{V}{N} = 1/n$ . Putting this all together into 2.14 we get:

$$\left( \frac{\partial f(T, n)}{\partial V} \right)_{N, T} \cdot \frac{1}{n} \cdot \frac{V}{\mu} = -1 \quad (2.15)$$

Finally we can use eq. 2.15 inside eq. 2.13 to achieve the following:

$$P = f + V \cdot \left( \frac{n \cdot \mu}{V} \right) = f - n \cdot \mu \quad (2.16)$$

Having a simplified result for pressure, we can now apply the coexistence constraint that  $P_1 = P_2 \Rightarrow f_1 + n_1 \cdot \mu = f_2 + n_2 \cdot \mu$ . To compare this result with eq. 2.12, solve for  $\mu$  to get the following results:

$$\mu = \frac{f_2 - f_1}{n_2 - n_1} \quad (2.17)$$

$$\text{from eq. 2.12: } \mu = \left( \frac{\partial f(T, n)}{\partial n} \right)_{T, V_1} \Big|_{n_1} = \left( \frac{\partial f(T, n)}{\partial n} \right)_{T, V_1} \Big|_{n_2} \quad (2.18)$$

The above constraints indicate that coexistence only occurs when the average slope must be equal to the instantaneous slope. This is equivalent to plotting the free energy as a function of density and finding a common tangent.

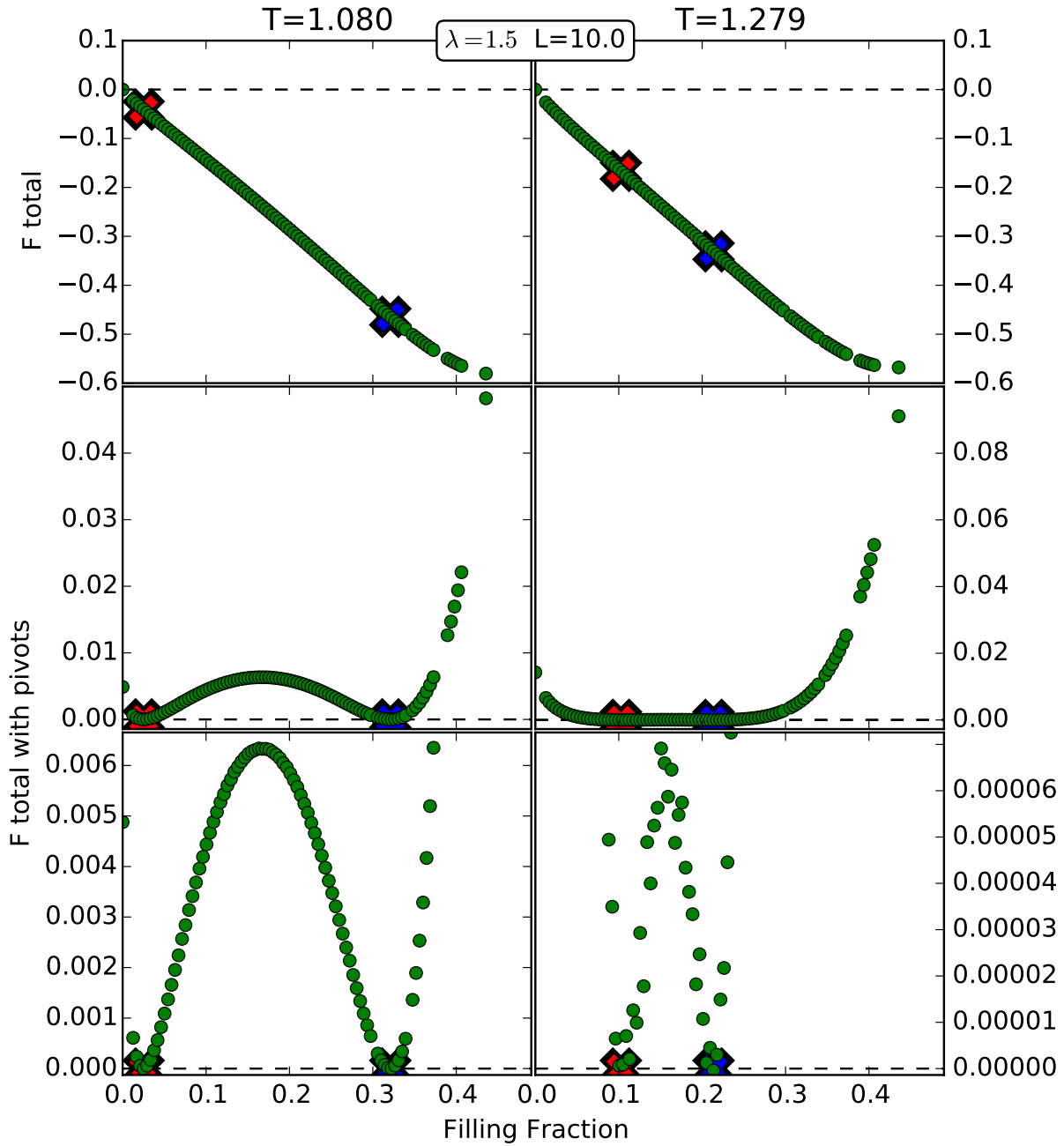


Figure 2.2: Here the common tangent method is demonstrated. The free energy at a particular temperature is plotted as a function of density. The two points highlighted by red and blue X's on the curve share a common tangent; this means both points will have the same pressure and chemical potential. The left and right set of plots shows how the signal to noise ratio changes as the temperature increases. Far from the critical point the signal is relatively strong, while near the critical point the noise becomes significant. To prevent the loss of the signal, first start at a low temperature where the signal is strong. Then gradually increase the temperature while finding common tangents. As the temperature and noise increases, the previous solutions at a slightly lower temperature can be used as a guess for the new higher temperature.

# Results

## Trends in U,F

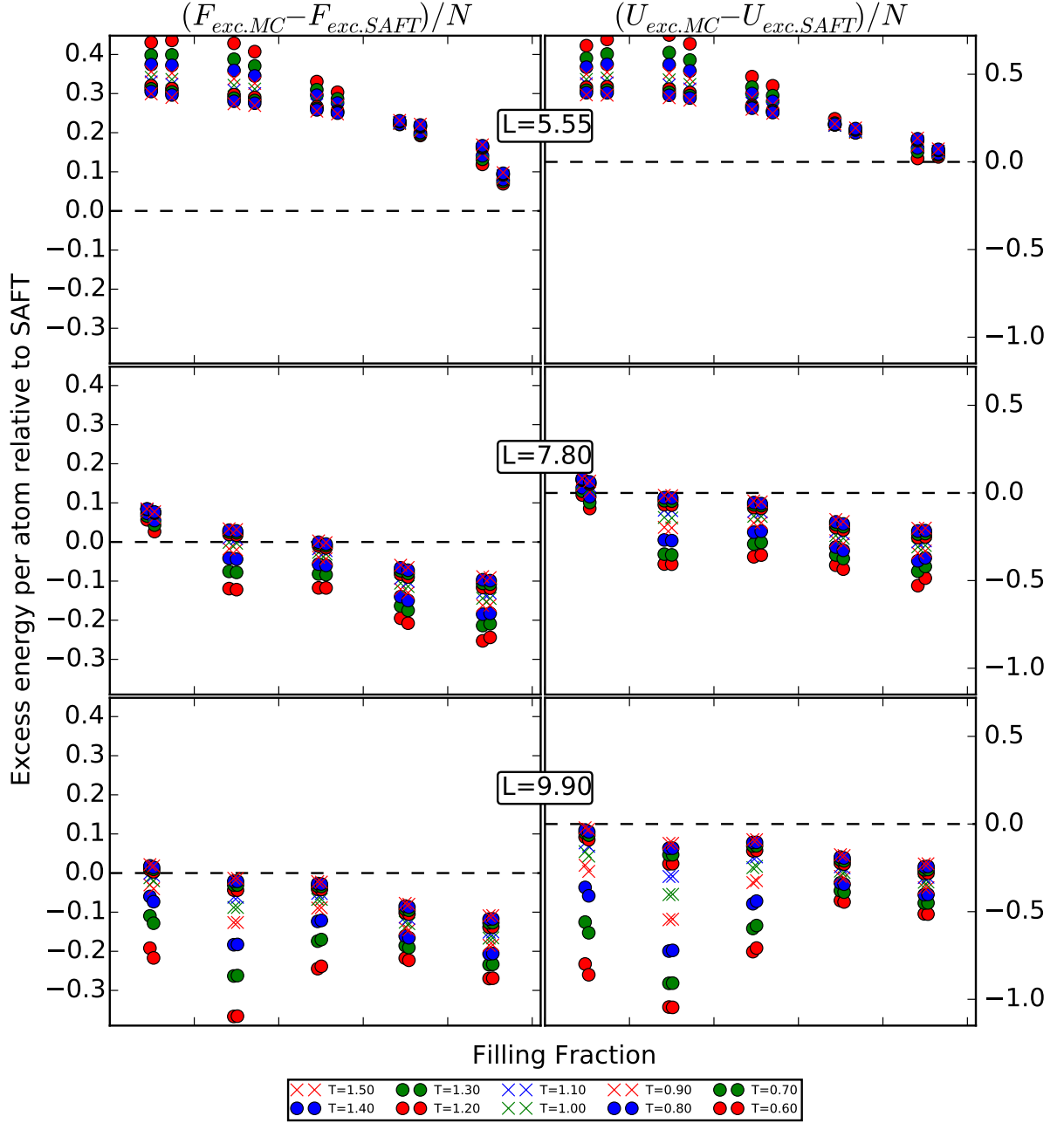


Figure 3.1: These graphs show the Monte Carlo simulation results in terms of dispersive free energy and internal energy relative to SAFT at three different box sizes. Both sets of graphs show that a small box size has a higher energy than SAFT, while a larger box will have a lower energy than SAFT. This makes sense because as the box size increases longer wavelength fluctuations are allowed, and these longer wavelengths actually lower the allowed energy as the increase in energy due to the low density regions are more than compensated by the decrease in energy due to the high density regions. Given a constant box size, the high filling fraction simulations cannot fluctuate as much as the low filling fraction simulations, which explains the bulge in the two lower plots.



## Trends in S,Cv

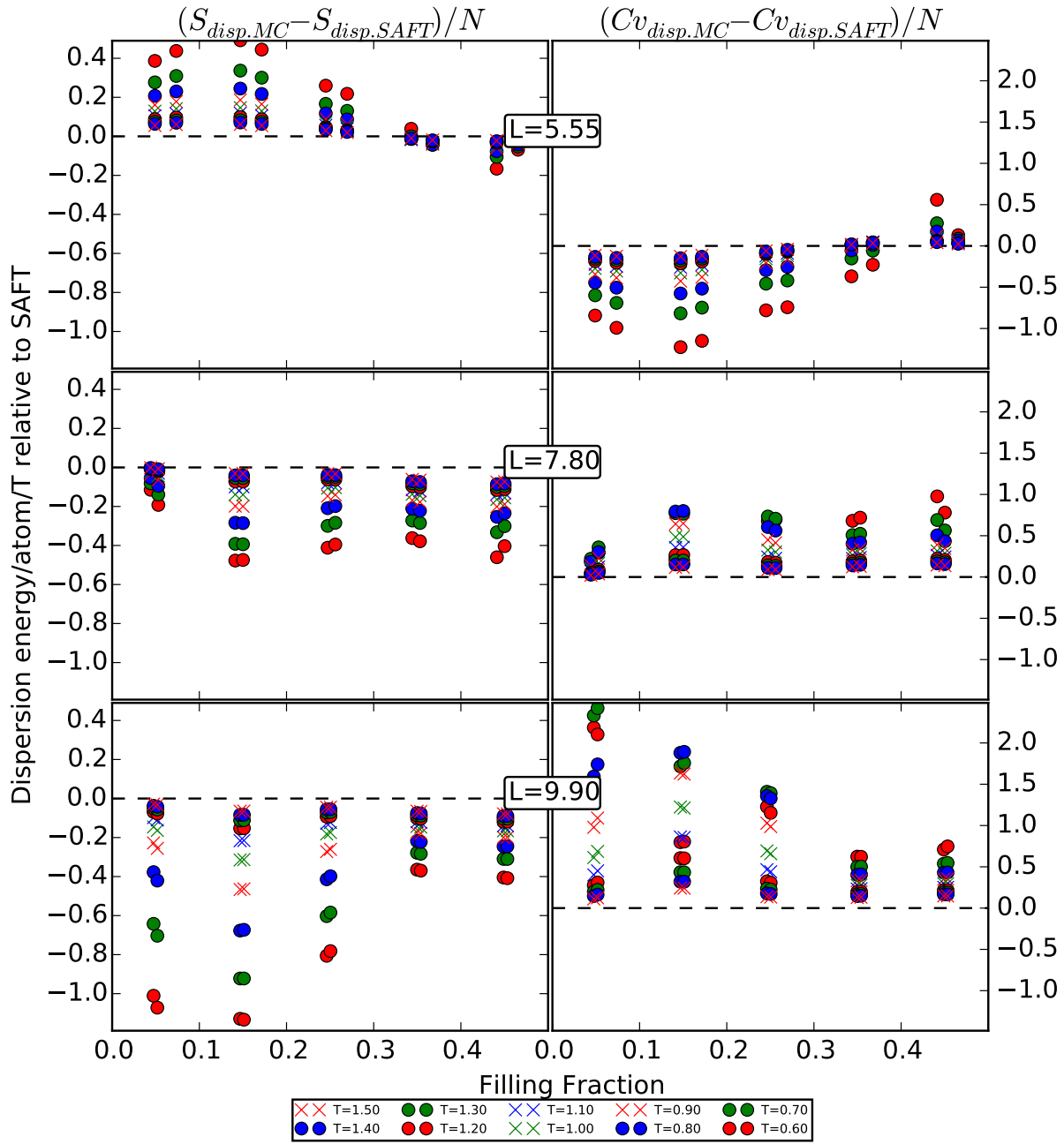


Figure 3.2: These graphs show the Monte Carlo simulations results in terms of dispersive entropy and heat capacity per particle relative to SAFT at three different box sizes. It is interesting to see the entropy trends are nearly the inverse of the heat capacity trends. Both entropy and heat capacity require a derivative to find, it is just that entropy is the negative derivative of Free energy while heat capacity is the positive derivative of internal energy. Given fig. 3.1 showed the internal energy had the same trend as the free energy, it isn't surprising entropy and heat capacity have inverse trends. Regarding the trend itself, the graphs suggest entropy of a small box will have more entropy than SAFT, while a large box will have a lower entropy than SAFT. This trend can be explained by the particles binding together in ways that SAFT could not take into account, and this extra binding will decrease the entropy simply because some states are now favored over other states.

### Using Cost to Estimate Best Box Size

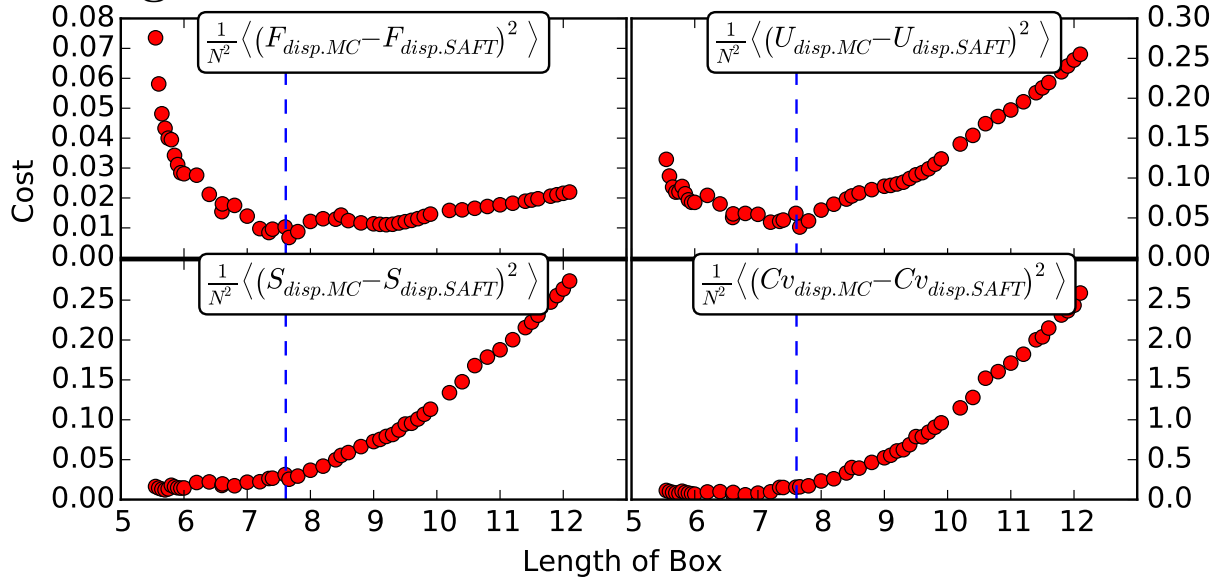


Figure 3.3: These graphs show the cost function as a function of the box size for the dispersive free energy, internal energy, entropy, and heat capacity. The cost function is defined as the mean square difference between the Monte Carlo simulations and SAFT evaluated at a filling fraction of [0.15,0.25,0.35,0.45] and evaluated for  $0.6 < T < 1.5$ . The dispersive free energy and internal energy show a minimum near  $L=7.6$ , while any box size less than  $L=8.0$  seems to be just fine for the dispersive entropy and heat capacity.

### Coexistence: T vs Density

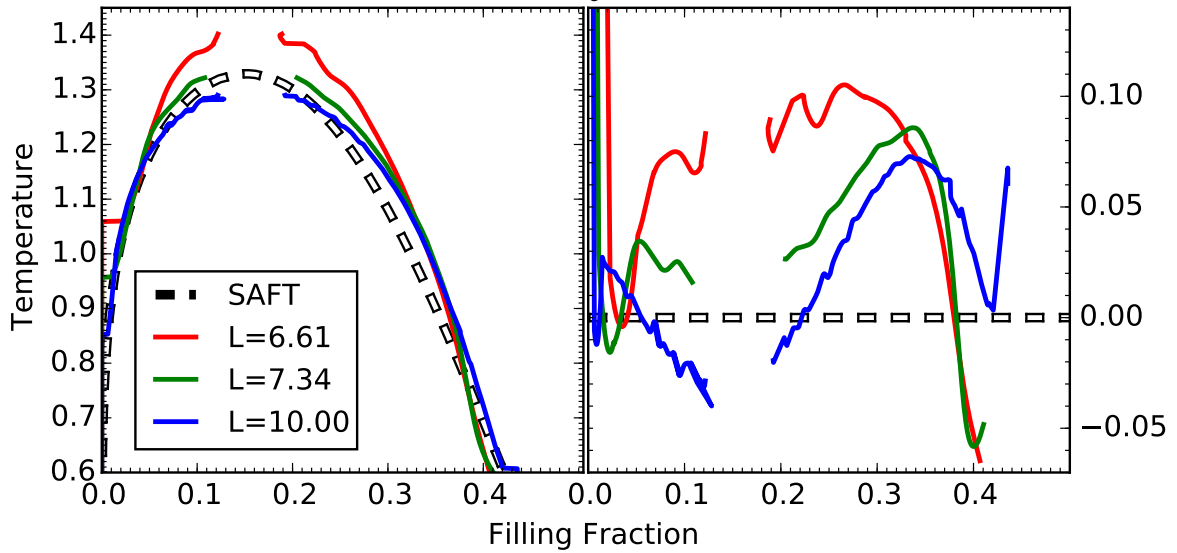


Figure 3.4: Here the gas-liquid coexistence temperature as a function of filling fraction for three different Monte Carlo simulations are compared to SAFT. The box size  $L=6.61$  clearly has a higher critical temperature than SAFT, while the box size  $L=10.00$  clearly has a lower critical temperature than SAFT.

# Conclusion

## Conclusion

ta-da!